UNIVERSITY OF MINNESOTA
ST. ANTHONY FALLS LABORATORY
Engineering, Environmental and Geophysical Fluid Dynamics

Project Report No. 517

A flow and temperature model for the Vermillion River, Part I: Model development and baseflow conditions

by

William Herb and Heinz Stefan

Prepared for

Minnesota Pollution Control Agency
St. Paul, Minnesota

August 2008
Minneapolis, Minnesota

The University of Minnesota is committed to the policy that all persons shall have equal access to its programs, facilities, and employment without regard to race, religion, color, sex, national origin, handicap, age or veteran status.

Abstract

Stream temperature and stream flow are important physical parameters for aquatic habitat preservation in river and stream systems. Water temperature is particularly important for coldwater stream systems that support trout. Summer base flow conditions with low flows and high water temperatures can be critical for maintaining trout habitat. Surface runoff from rainfall events can lead to increases in stream temperature, particularly in developed watersheds. To better understand the interactions between stream temperature, land use, and climate, an unsteady stream flow and temperature model has been developed for the Vermillion River.

The model includes the main stem from Dodd Avenue to Goodwin Avenue and a number of tributaries, including South Branch, South Creek, North Creek, and Middle Creek. The EPD-riv1 package was used to simulate stream flow, including distributed groundwater inputs. Simplified stream channel geometry was required to obtain converged flow solutions for unsteady low flows. A stream temperature model has been assembled based on previous work at SAFL. The stream temperature model uses flow and flow area from the flow solver, along with observed climate data to calculate surface heat transfer. Groundwater inflows are an important component of both the flow and temperature model. For the Vermillion River, groundwater inflow rates were estimated from flow gaging sites, while groundwater temperatures were estimated by calibrating the stream temperature model. The calibrated combination of groundwater flow and temperature results in a good match of simulated and observed stream temperature, with RMSEs in the range of 0.75 to 2 ºC.

The assembled flow and temperature model for the Vermillion River has been calibrated for baseflow conditions, and provides a starting point for future analysis of surface runoff inputs during rainfall events.

Table of Contents

1. Introduction

Stream temperature and stream flow are important parameters for aquatic habitat preservation in river and stream systems. Water temperature is particularly important for coldwater stream systems that support trout. Summer base flow conditions with low flows and high water temperatures can be critical for maintaining trout habitat. Surface runoff from rainfall events can lead to increases in stream temperature, particularly in developed watersheds. To better understand the interactions between stream temperature, land use, and climate, an unsteady stream flow and temperature model has been developed for the Vermillion River. This river is at the southern fringes of the Twin Cities metropolitan area (Figure 1.1) and has a world-class brown trout fishery.

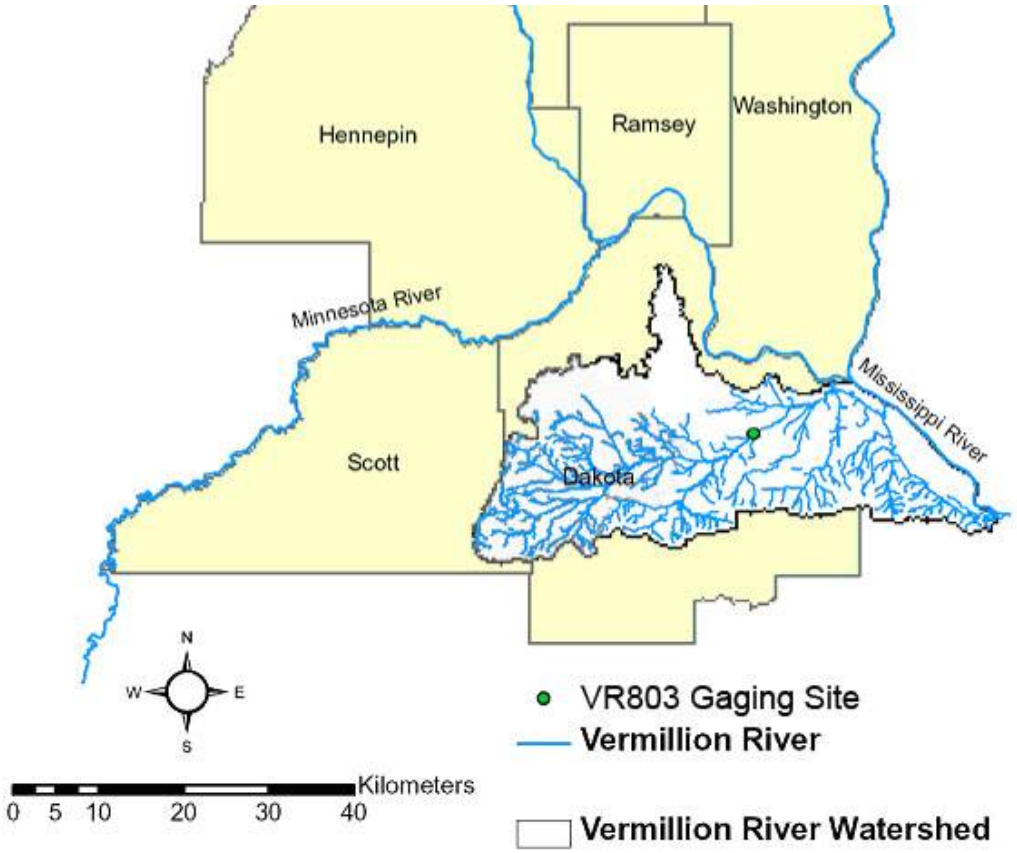

Figure 1.1. The Vermillion River watershed in Scott and Dakota counties. The study area includes the Vermillion River main stem and major tributaries upstream of the VR803 station, near the town of Vermillion, MN.

The flow and temperature model is designed to simulate the response of the river to surface runoff inputs, however, the model can be run for continuous analysis of several months. Stream flow is simulated at 1 to 5 minute time steps, while stream temperature is simulated at 15 minute to 1 hour time steps, using observed climate data as the primary input. Groundwater inputs (flow per unit length and temperature) are also included, and are an important part of the flow and temperature simulations. In addition to detailed temperature and flow time series, the model provides broad scale characterizations of heat transport in the Vermillion, including the relative

importance of groundwater temperature, atmospheric heat transfer, and surface water inputs in determining stream temperature. The stream temperature model can therefore be used as a tool to determine what management practices (e.g. stormwater BMPs, bank shading, groundwater conservation) are best to maintain cold water temperatures for trout habitat. This report describes the model formulation and calibration for baseflow conditions. The response of the river to surface runoff inputs will be described in a later report.

2. Stream flow Model

The extent of the flow and temperature model includes the main stem from Dodd Avenue to Goodwin Avenue, along with sections of major tributaries, including North Creek, Middle Creek, South Branch, and South Creek (Figure 2.1).

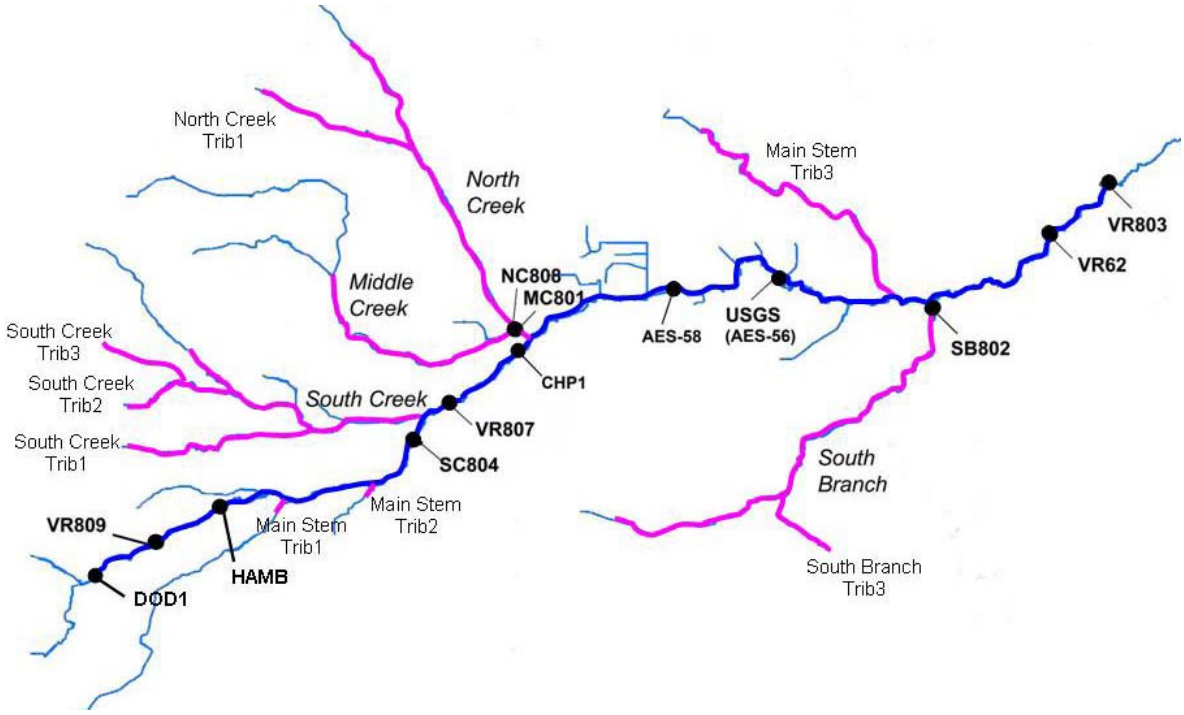

Reach	Length (km)	Average Slope (m/m)	Reach	Length (km)	Average Slope (m/m)
Main Stem	46.4	0.001	South Branch Trib1	2.5	0.0028
Main Stem Trib3	10.7	0.0027	South Creek	8.8	0.0029
Middle Creek	5.6	0.002	South Creek Trib1	5.7	0.0046
North Creek	7.1	0.0015	South Creek Trib2	2.9	0.0041
North Creek Trib1	2.9	0.002	South Creek Trib3	1.6	0.0049
South Branch	14.4	0.0015			

Figure 2.1. Extent of the flow and temperature model for the Vermillion River main stem (dark blue line) and tributaries (pink lines). The upstream end (DOD1) is Dodd Boulevard, while the downstream end (VR803) is Goodwin Avenue. Main stem Trib1 and Trib2 are specified flow input points to the main stem model, but these tributaries are not modeled separately.

2.1 Main Stem of the Vermillion River

2.1.1 Model development

A stream flow model for the main stem of the Vermillion was created for a channel length of approximately 29 miles, between Dodd Boulevard (south of the Lakeville airport) and Goodwin Avenue, just east of the town of Vermillion. The stream geometry for the main stem was supplied to SAFL by Barr Engineering, in HEC-RAS and HEC-2 format, with about 240 channel and floodplain cross-sections, and detailed descriptions of bridges and culverts. Main stem stream geometry was obtained for stations between Dodd Blvd and Goodwin Avenue. The flow analysis for this study differs from previous flow analysis of the Vermillion in that previous studies were focused on flood analysis, while this study is focused on mid-summer baseflow condition and the response to small to moderate storm events.

The flow analysis of the main stem was started by performing unsteady flow analysis within the HEC-RAS package (USACE 2008). While steady baseflow conditions can be handled with steady-state flow analysis, the flow model is ultimately required to simulate the unsteady response of stream flow to surface runoff inputs, therefore, the ability of HEC-RAS to handle unsteady flow starting from a low baseflow condition was immediately investigated. In initial testing, it was apparent that the HEC-RAS unsteady flow analysis had difficulty converging for flows below about 20 cfs, and some converged solutions had much higher velocities (15-20 ft/sec) than steady state flow solutions for the same flow rate. Since the upper portions of the main stem often have baseflows of 1 to 10 cfs, several modifications to the model were investigated to improve the ability to handle low flows:

1. Additional cross sections were added, interpolating between existing cross-sections. This appeared to give little benefit.
2. The bridges and culverts were removed from the model to simplify the channel geometry, reasoning that the flow restrictions of these structures are less important at lower flows. This slightly improved the ability to handle low flows.
3. The channel cross-sections were simplified. Simple parabolic shapes were fit to each of the surveyed channel cross-sections (Figure 2.1), and a smooth variation in the channel aspect ratio from upstream to downstream was created to best fit the variation in observed channel cross-sections. The surveyed channel bottom elevations were maintained. This simplified channel geometry enabled greatly improved low flow solutions, with reasonable simulations down 1-2 cfs.
4. In steady flow simulations of some stream reaches, irregularities in the surveyed channel bottom points caused overbank flows to be predicted at baseflow conditions, e.g. 2 – 10 cfs. These predicted flow conditions appeared to be unrealistic. As a correction, the surveyed channel bottom elevations were smoothed with a second to third order polynomial in all stream reaches.
5. A second analysis package was evaluated, the EPD-Riv1 model, using the simplified channel geometry. The EPD-Riv1 model was found to have similar capabilities to HEC-RAS for unsteady flow analysis at low flows.

To evaluate the consequences of using the simplified geometry, an analysis was performed using both the simplified stream channel geometry and the original geometry for a case where the full

model converged. An input pulse of 20 to 40 cfs was specified at the upstream end, and the response of the models at the downstream end were compared (Figure 2.3). The EPD-Riv1 model (USEPA 2005) was also run with the simplified geometry for this case. All three models (HEC-RAS full geometry, HEC-RAS simplified geometry, EPD-Riv1 simplified geometry) gave very similar responses to the input pulse, indicating that the simplified geometry is a reasonable approach for this study. The use of the simplified geometry should be limited to bankfull discharge, however, since the stream geometry for overbank conditions will not be represented, and flow restrictions due to bridges and culverts will become more important for bankfull and overbank flows.

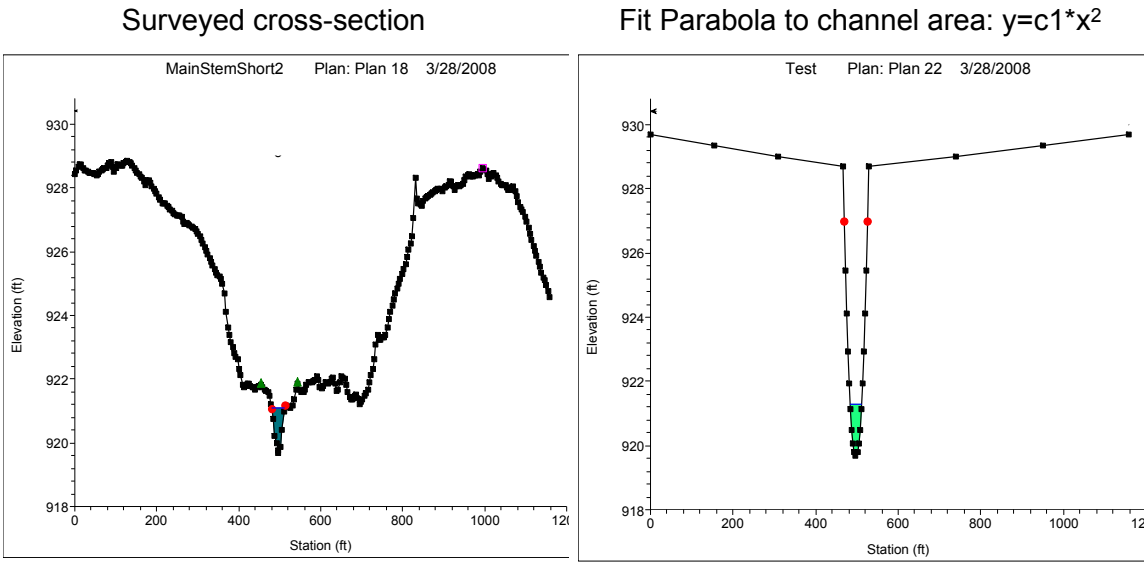

Figure 2.1. Example of a surveyed cross-section and a simplified, parabolic cross-section. The parabola was fit to the channel area between bank stations, and then extended upward to ensure that iterating flow solutions do not overflow the parabolic region.

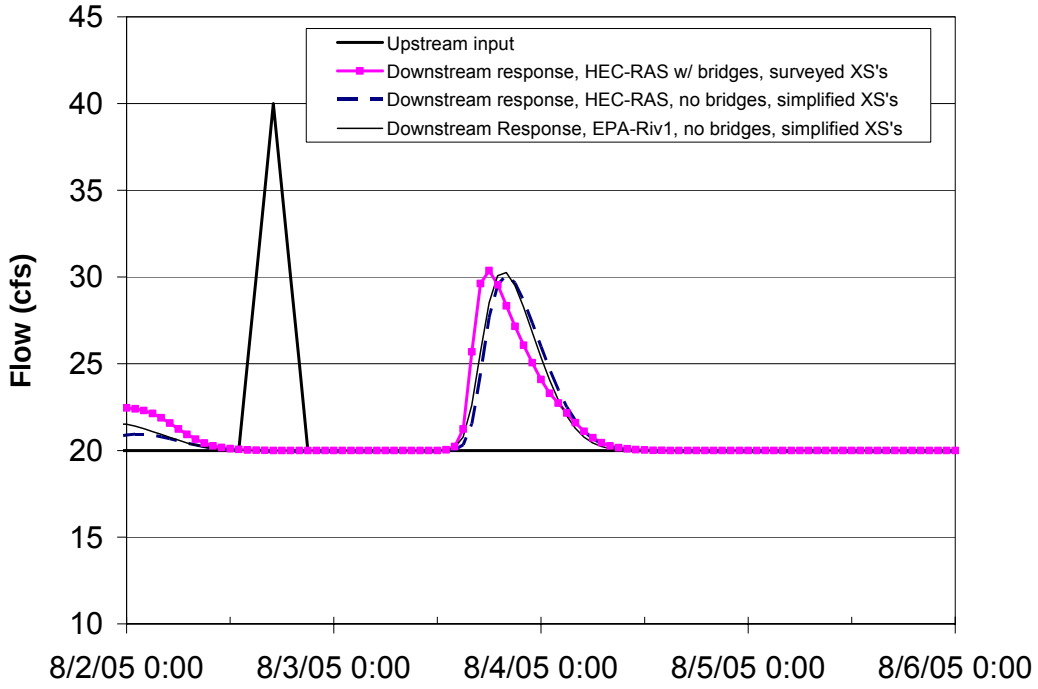

Figure 2.3. Simulated response of the main stem of the Vermillion to an input pulse at Hamburg Ave. of 20 to 40 cfs for the HEC-RAS and EPD-Riv1 models.

2.1.2 Baseflow Scenario for the Vermillion River Main Stem

Using the assembled geometry for the main stem, a mid-summer baseflow scenario was created based on observed 2006 flow data to provide a calibration flow condition for the temperature model. A baseflow scenario was created for the period August 9 to September 8, 2006. This period includes several rainfall events greater than 0.5 in, but no major precipitation and runoff events (Figure 2.4). Flow gaging data for Hamburg Avenue are not available for 2006 and 2007. The flow at Hamburg Avenue (Hamb) was estimated to be 1.2 cfs based the flow at SC804 (3.3 cfs), and a relationship developed between SC804 and Hamburg using 2005 data (Figure 2.5). Main stem Trib1 and Trib2 flows were set based on 2005 point flow measurements by the Dakota County SWCD. Tributary inflows were set to be a fraction of the flow at the USGS main stem station at Empire, based on summer monthly-averaged flows at tributary gaging stations (Herb and Stefan 2008), as given in Table 2.1. Groundwater inflows were uniformly distributed over three reaches of the main stem (Table 2.2), based on monthly-averaged flow differences between gaging stations (Herb and Stefan 2008). The flow inputs to the main stem are summarized in Table 2.1 and 2.2. A longitudinal distribution of flow for this period is given in Figure 2.6, clearly showing step increases due to tributaries and upward trends due to distributed groundwater inputs.

Table 2.1. Specified upstream and tributary flow inputs for the main stem of the Vermillion River for the August /September 2006 baseflow scenario.

Upstream and Tributary Flow Inputs	
Tributary	Flow Input (cfs)
Dod1 (upstream boundary)	0.25
Empire	13.3
Main Stem Trib1	1.0
Main Stem Trib2	0.7
Main Stem Trib3	0.25
North Creek (includes Middle Creek)	7.7
South Branch	6.7
South Creek	8.1

Table 2.2. Specified groundwater flow inputs for the main stem of the Vermillion River for the August /September 2006 baseflow scenario. RS 32.4 is 0.7 miles downstream of Hamburg Avenue.

Reach	Length (km)	Groundwater Input (cfs)	Groundwater Input Rate (cfs/mile)
DOD1 to VR809	2.56	0.0	0.0
VR809 to RS 32.4	3.60	1.4	0.39
RS 32.4 toVR807	10.32	0.0	0.0
VR807 to USGS	14.56	11.0	0.75
USGS to VR803	15.44	9.4	0.61

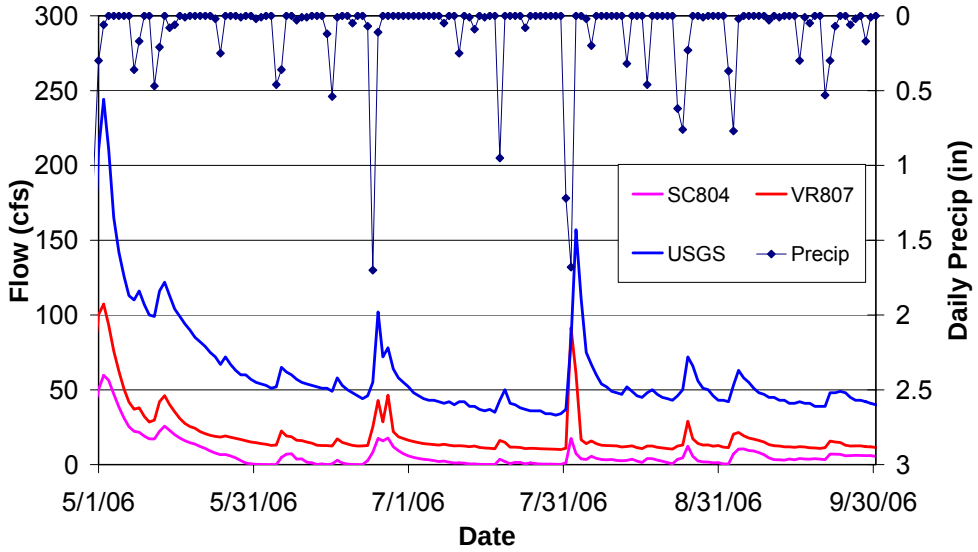

Figure 2.4. 2006 streamflow at three main stem stations (SC804, VR807, USGS) and daily precipitation from the Empire WWTP.

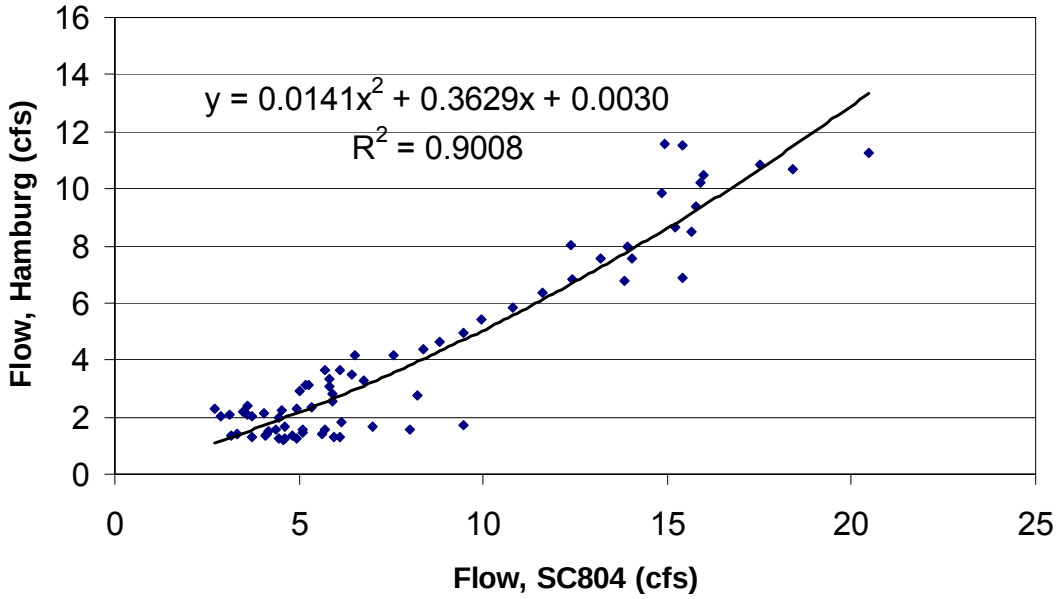

Figure 2.5. Relationship between daily average flows at SC804 and Hamburg Avenue, based on 2005 data.

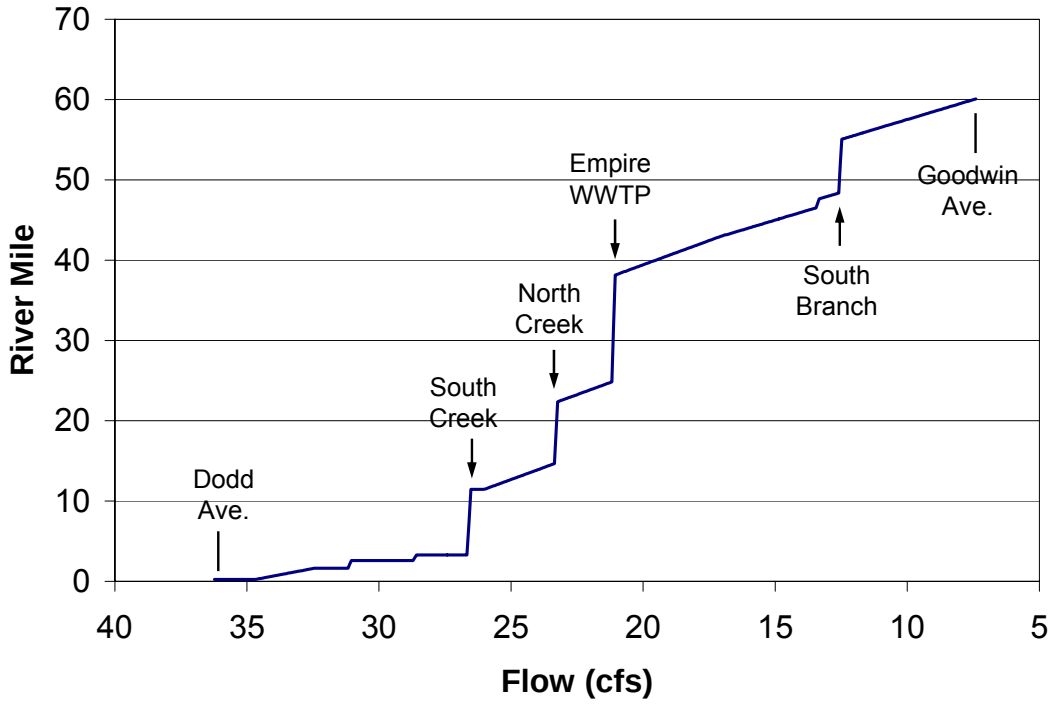

Figure 2.6. Simulated longitudinal distribution of flow in the main stem of the Vermillion River on August 1, 2005.

2.2 Flow models for Tributaries of the Vermillion River

A series of separate flow models were developed for tributaries of the Vermillion River, including North Creek, Middle Creek, South Creek, and South Branch (Figure 2.1). Channel geometry information available for all major tributaries, and one flow gaging station near the lower end of each tributary was available. The exception was South Creek, which is gaged indirectly via stations on the main stem upstream (SC804) and downstream (VR807) of the confluence with South Creek. Based on the flow analysis of the main stem, the HEC-RAS channel geometry for the tributaries was substantially simplified to enable unsteady, low flow solutions.

Table 2.3 summarized the specified upstream inputs and distributed groundwater flows for each reach. In most cases, there was no flow gaging for the upstream end of the tributary. A low value for the upstream input was assumed (0.25 cfs) and increased if necessary to enable unsteady flow analysis of simulated stormwater inputs. Groundwater inputs were adjusted to give known downstream flow values, or to give agreement in simulated and observed stream temperature at the downstream location. For the case of, e.g., South Creek Trib1, groundwater inputs needed to be concentrated near the downstream end of the each to produce the low observed stream temperature.

Table 2.3. Summary of specified upstream inputs and distributed groundwater flows for each tributary reach. The location of each tributary is shown in Figure 2.1.

Reach	Length (km)	Upstream Baseflow Input (cfs)	Groundwater Input (cfs)
Main Stem Trib1	10.7	0.25	0.25
Middle Creek	5.6	0.5	0.5
North Creek	7.1	0.5	5.25
North Creek Trib1	2.9	0.5	0.5
South Branch	14.4	0.5	5.1
South Branch Trib1	2.5	0.5	0.5
South Creek	8.8	0.25	5.6
South Creek Trib1	5.7	0.5	1.75
South Creek Trib2	2.9	0.25	0.4
South Creek Trib3	1.6	0.25	0.4

3. Stream Temperature Model

A 1-D model was developed to simulate stream temperature based on atmospheric heat transfer, sediment heat transfer, and groundwater inflows. It is based on previous stream temperature models developed at SAFL, e.g. the MNSTEM model (Sinokrot and Stefan 1993). The model is based on a finite difference formulation, solving for the variation of stream temperature as a function of time and streamwise distance, assuming the stream channel is well mixed vertically and laterally. Longitudinal transport of heat is assumed to be via advection only, neglecting dispersion. This limits the applicability of the present model to free-flowing river systems

without major pools, reservoirs, etc. Model inputs include climate parameters (air temperature, relative humidity, wind speed, and solar radiation), the channel geometry, streamflow values, lateral (tributary) inflow rates and temperature, groundwater inflow rates and temperatures, and shading/sheltering coefficients (Figure 3.1).

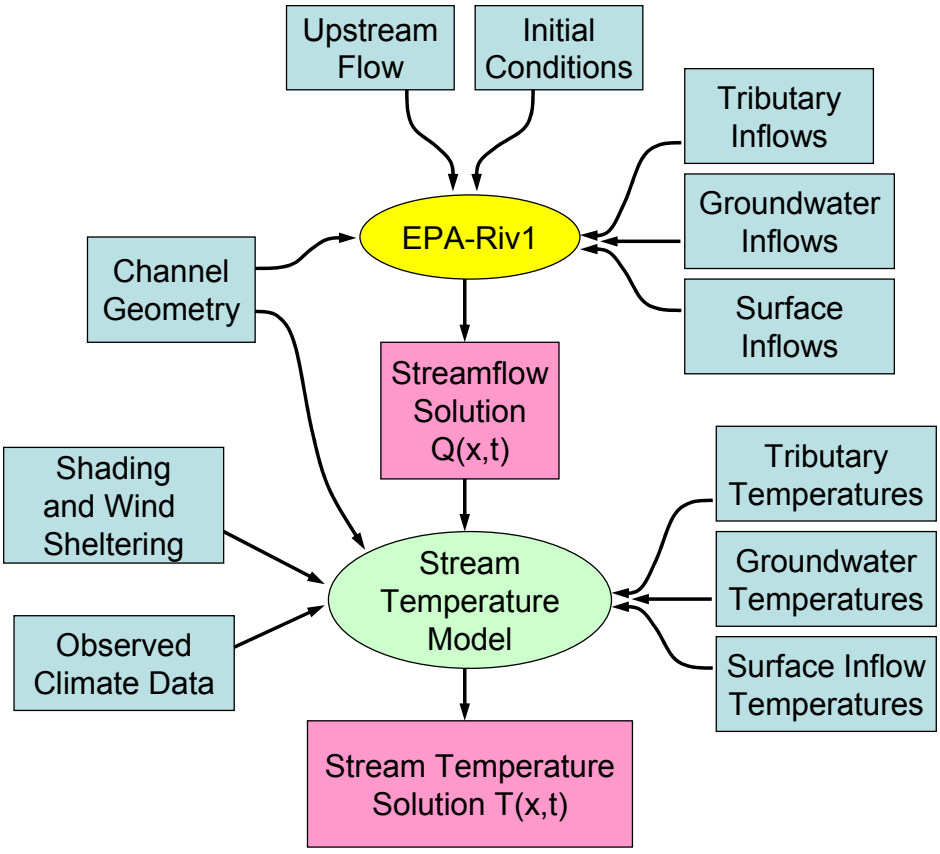

Figure 3.1. Flow chart summarizing the input data and simulation results for the flow and temperature solvers used in this study.

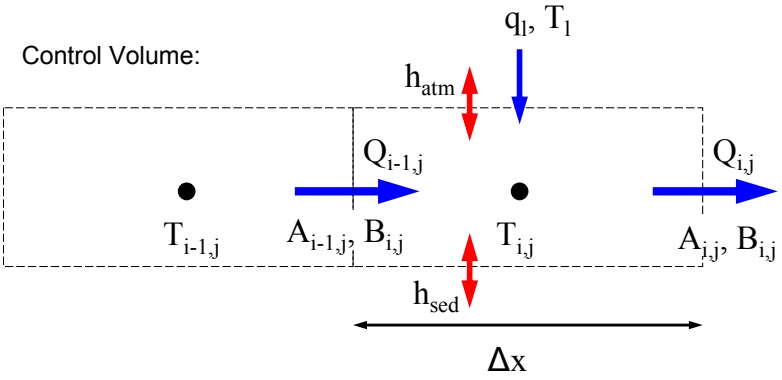

Figure 3.2. Schematic for mass and heat flows in and out of a stream channel control volume.

3.1 Stream Temperature Model Formulation

The stream temperature model is based on the unsteady, 1-D differential equation for the advective transport of a scalar (temperature), Equation 3.1. Longitudinal dispersion is neglected in this formulation. Lateral inflows and groundwater inflows are treated in the same way, as a specified lateral flow (q_l) and temperature (T_l) for each control volume. The parameter symbols are summarized in Table 3.1.

3.1 $$\frac{\partial}{\partial t}(AT)+\frac{\partial}{\partial x}(QT)=S$$

3.2 $$S=\frac{B\,h_{atm}}{\rho C_p}+q_l T_l+\frac{W_p\,h_{sed}}{\rho C_p}$$

The finite-difference discretization of Equations 3.1 and 3.2 is given in Equations 3.3 – 3.7. Stream flow values ($Q_{i,j}$) from an unsteady flow solution are supplied at the control volume faces, while temperature ($T_{i,j}$) is solved for at the center of each control volume (Figure 3.2). The discretization schemes used for the derivative terms in Equation 3.1 were chosen to match the discretization used for the flow solution in the EPD-Riv1 model, so that flow solutions obeying continuity in EPD-Riv1 would also obey continuity in the temperature model. In the EPD-Riv1 model, each specified lateral flow input is split between two cells, based on the relative length of each cell. Equation 3.5 was used to calculate an equivalent lateral flow input (q_l) for each cell in the temperature model, based on the specified lateral inflows used in the EPD-Riv1 model. This was a necessary step to ensure mass continuity was maintained in the temperature model.

3.3 $$\frac{\partial}{\partial t}(AT)=\frac{1}{2\Delta t}\left(A_{i-1,j+1}T_{i-1,j+1}+A_{i,j+1}T_{i,j+1}+A_{i-1,j}T_{i-1,j}-A_{i,j}T_{i,j}\right)$$

3.4 $$\frac{\partial}{\partial x}(QT)=\frac{1}{\Delta x}\left(Q_{i,j+1}T_{i,j+1}-Q_{i-1,j+1}T_{i-1,j+1}\right)$$

3.5 $$q_{l_i}=q^*_{l_{i-1}}\frac{\Delta x_{i-1}}{\Delta x_i+\Delta x_{i-1}}+q^*_{l_i}\frac{\Delta x_i}{\Delta x_i+\Delta x_{i+1}}$$

3.6 $$S=\frac{\overline{B}\left(h_{atm}+h_{sed}\right)}{\rho C_p}+q_l T_l$$

3.7 $$\overline{B}_i=\frac{B_{i-1,j}+B_{i,j}+B_{i-1,j+1}+B_{i,j+1}}{4}$$

The stream temperature model described here is used in conjunction with flow data supplied by the EPD-Riv1 model. The lateral (q_l) and instream (Q_i) flows are transferred as text files from the flow solution to the stream temperature model. The need to additionally transfer the flow areas (A_i) for each node is eliminated by calculating the flow areas in the stream temperature solver using Equation 3.8. Flow areas for the first time step are transferred from the flow solver

as an initial condition. While this method eliminates the need to transfer flow area data for each time step, it does require that the flow data be transferred with at least 5 to 6 significant digits to avoid cumulative errors in the mass balance and the flow areas, particularly for low flows.

$$3.8 \quad A_{i,j+1} = A_{i,j} + A_{i-1,j} - A_{i-1,j+1} + \frac{2\,\Delta t}{\Delta x_i}\left(Q_{i-1,j+1} + ql_{i,j+1} - Q_{i,j+1}\right)$$

Inserting Equations 3.3 – 3.7 into Equation 3.1 gives the final equations that are used to solve for the stream temperatures for each cell and each time step:

$$3.9 \quad C_1\,T_{i,j+1} = C_2\,T_{i-1,j} + C_3\,T_{i-1,j+1} + C_4 T_{i,j} + C_5$$

$$3.10 \quad C_1 = A_{i,j+1} - \frac{2\,\Delta t\,Q_{i,j+1}}{\Delta x_i} - \frac{2\,\Delta t\,\overline{B}_i}{\rho C_p}\left(\frac{\partial h_{atm}}{\partial T} + \frac{\partial h_{sed}}{\partial T}\right)$$

$$3.11 \quad C_2 = A_{i-1,j}$$

$$3.12 \quad C_3 = -A_{i-1,j+1} + \frac{2\,\Delta t\,Q_{i-1,j+1}}{\Delta x_i}$$

$$3.13 \quad C_4 = A_{i,j} - \frac{2\,\Delta t\,\overline{B}_i}{\rho C_p}\left(\frac{\partial h_{atm}}{\partial T} + \frac{\partial h_{sed}}{\partial T}\right)$$

$$3.14 \quad C_5 = \frac{2\,\Delta t\,\overline{B}_i}{\rho C_p}\left(h_{atm} + h_{sed}\right) + 2\,\Delta t\,q_l T_l$$

Table 3.1 Parameter Definitions

Symbol	Definition and units
A	flow cross-sectional area (m^2)
B	stream width (m)
h_{atm}	atmospheric heat transfer rate (W/m^2)
h_{sed}	sediment heat transfer rate (W/m^2)
i	cell number index (streamwise direction)
j	time step index
q_l	lateral inflow (m^2/s) in the stream temperature model
q^*_l	lateral inflow (m^2/s) in the EPD-Riv1 flow solver
Q	flow rate (m^3/s)
S	heat source term ($ºC \cdot m^2/s$)
t	time (s)
T_l	lateral inflow temperature (ºC)
T	temperature (ºC)
W_p	wetted perimeter ≈ stream width (m)
x	streamwise distance (m)
ρCp	density · specific heat (J/m^3)
Δt	time step (s)

Both h_{atm} and h_{sed} have a nonlinear dependence on stream temperature. The atmospheric heat transfer is calculated based on the current climate conditions (air temp, humidity, wind, solar radiation, cloud cover) and the current stream temperature, as detailed in Appendix I. The vertical profile of sediment temperature and the sediment heat flux (h_{sed}) is determined for each stream node at each time step using the formulations given in Appendix II. 10 to 12 nodes are typically used in the sediment temperature model, with closer node spacing near the sediment/water interface. To improve the numerical stability of the solution, both the atmospheric heat transfer and sediment heat transfer terms are linearized, by evaluating both the heat flux and the derivative of the heat flux at the current stream temperature T_j:

$$3.15 \quad h_{atm}\left(T_j, T_{j+1}\right) = h_{atm}\left(T_j\right) + \frac{h_{atm}\left(T_j + \delta T\right) - h_{atm}\left(T_j\right)}{\delta T}\left(T_{j+1} - T_j\right)$$

$$3.16 \quad h_{sed}\left(T_j, T_{j+1}\right) = h_{sed}\left(T_j\right) + \frac{h_{sed}\left(T_j + \delta T\right) - h_{sed}\left(T_j\right)}{\delta T}\left(T_{j+1} - T_j\right)$$

Table 3.2. Parameter symbols and values used in surface heat transfer model.

	Description	Nominal Value
C_{fc}	forced convection transfer coefficient	0.0014
C_{nc}	free convection transfer coefficient	0.0015
CS_h	wind sheltering coefficient for heat transfer	1.5
α	surface albedo	0.087
β	fraction of solar radiation absorbed at the water surface	0.4
ε	water emissivity	0.97

3.2 Temperature Model for the Main Stem of the Vermillion River

A stream temperature model was assembled for the Vermillion River main stem from Dodd Blvd. to Goodwin Avenue. The model included 469 stations over a reach length of 28.8 miles (46.3 km), giving a station spacing of about 100 m. The stream station positions and tributary input locations were determined from the original HEC-RAS geometry. The stream temperature model for the main stem uses the same number of nodes as the flow model (Section 2.1), but the temperature nodes are offset from the flow solution nodes, with flows specified at the boundaries of the control volumes and temperatures calculated at the center of control volumes (Figure 3.2).

The geometry parameters used include the flow area and the top width of the stream. The simplified, parabolic cross-sections used for the flow solution (Section 2.1) were used to calculate the stream width (B) based on the calculated flow area (A) for each station:

$$(3.17) \quad B = C_B A^{1/3}$$

where C_B is a constant based on the parabolic shape used to describe the stream cross-section. C_B was adjusted to give an approximate match of the simulated stream width (from the flow solver) to the observed stream width from aerial photographs. C_B is used in both the flow and temperature solutions.

Model Calibration for Baseflow Conditions

The main stem stream temperature model was calibrated for the period August 9, 2008 to September 8, 2008. Calibration parameters included the shading and wind sheltering coefficients, and the flow rate and temperature of groundwater inputs. For the calibration period, 10 observed 15 minute stream temperatures were available for the main stem (Figure 3.3). Climate data used for the simulation included 1 hour air temperature, dew point, and wind speed from the Lakeville (Airlake) airport and 30 minute solar radiation data from the UofM Rosemount Experimental Station (Figure 3.4).

Each stream temperature observation point (Figure 3.3) provided the opportunity to calibrate the shading, sheltering, and groundwater parameters for a reach segment. The shading and sheltering coefficients were set to obtain the best match of simulated and observed diurnal temperature change. The groundwater flow rate was set for each reach based on the baseflow scenario developed for the period, described in Section 2.2. For the main stem, the groundwater temperature for each reach was then set to obtain the best match of simulated and observed daily mean stream temperature. The groundwater flow rates and calibrated groundwater temperatures are summarized in Table 3.3.

Tributary input temperatures were initially set equal to the observed temperature for the period. The observed tributary temperatures were then replaced with simulated temperatures as the stream temperature models for the tributaries were completed and calibrated. Observed stream temperatures were not available for main stem Trib1 and Trib2, and models were not constructed for these tributaries. Observed stream temperature from the Hamburg Avenue location were used to represent the temperature of Trib1 and Trib2 in all cases.

Table 3.3. Calibrated shading and wind sheltering coefficients for the main stem of the Vermillion River.

Station	Shading Coefficient	Sheltering Coefficient
Hamburg	0.85	0.85
SC804	0.70	0.70
VR807	0.5	0.6
CHP1	0.75	0.75
BSC2	0.3	0.4
AES-58	0.3	0.4
AES-56	0.5	0.6
AES-109	0.52	0.59
VR803	0.20	0.30

Table 3.4. Specified groundwater temperatures for the main stem of the Vermillion River for the August /September 2006 baseflow scenario. RS 52.1 is approximately 1.1 km downstream of Hamburg Avenue. Flow values are repeated from Table 2.2.

Reach	Groundwater Input (cfs)	Groundwater Temperature (ºC)
DOD1 to VR809	0.0	n/a
VR809 to RS 52.1	1.4	12.0
RS 52.1 toVR807	0.0	n/a
VR807 to USGS	11.0	14.0
USGS to VR803	9.4	14.0

Table 3.5. Calibrated shading and wind sheltering coefficients for the main stem of the Vermillion River, and the RMSE (root-mean-square error) of simulated stream temperature for the period August 9 to September 8, 2006.

Station	Shading Coefficient	Sheltering Coefficient	RMSE (ºC)
Hamburg	0.85	0.85	2.0
SC804	0.70	0.70	0.7
VR807	0.5	0.6	1.1
CHP1	0.75	0.75	0.9
BSC2	0.3	0.4	1.2
AES-58	0.3	0.4	1.0
AES-56	0.5	0.6	
AES-109	0.52	0.59	0.7
VR803	0.20	0.30	1.1

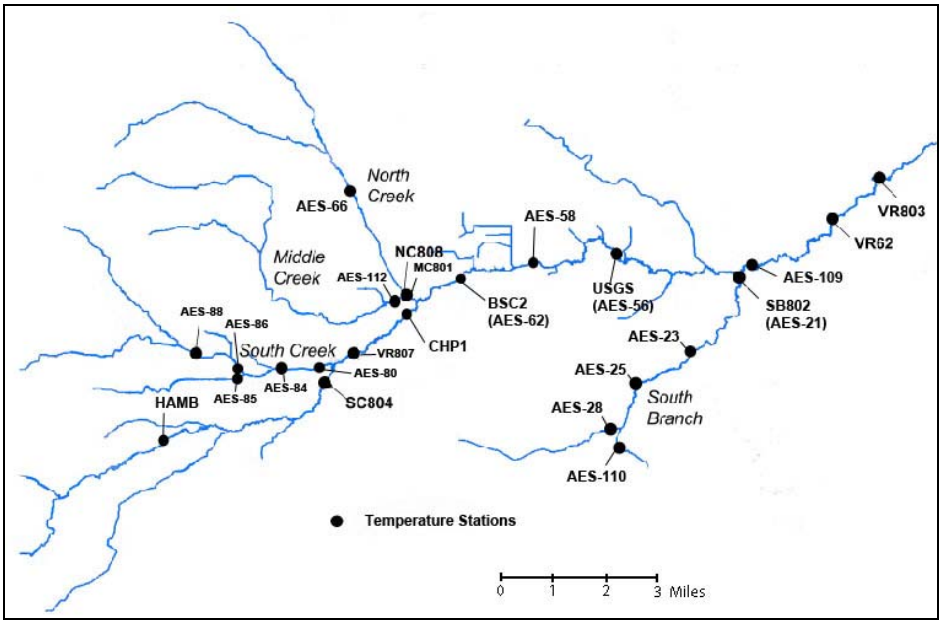

Figure 3.3. Vermillion River stream temperature measurement stations.

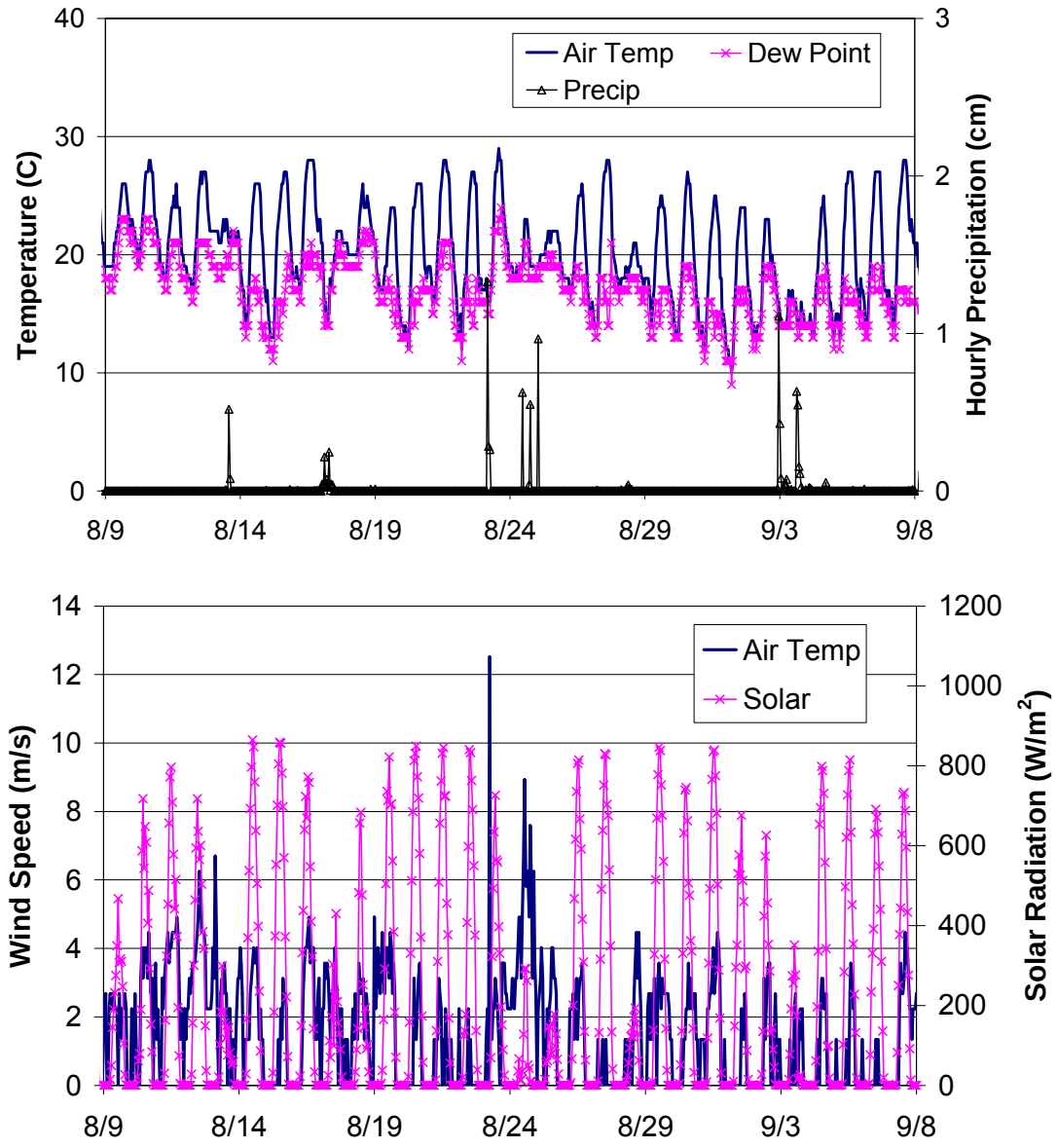

Figure 3.4. Observed climate data from the Lakeville Airport (air temp, dew point, wind speed) and the UofM Experimental Ag Station (solar radiation, precipitation) for the period August 9 to September 8, 2006.

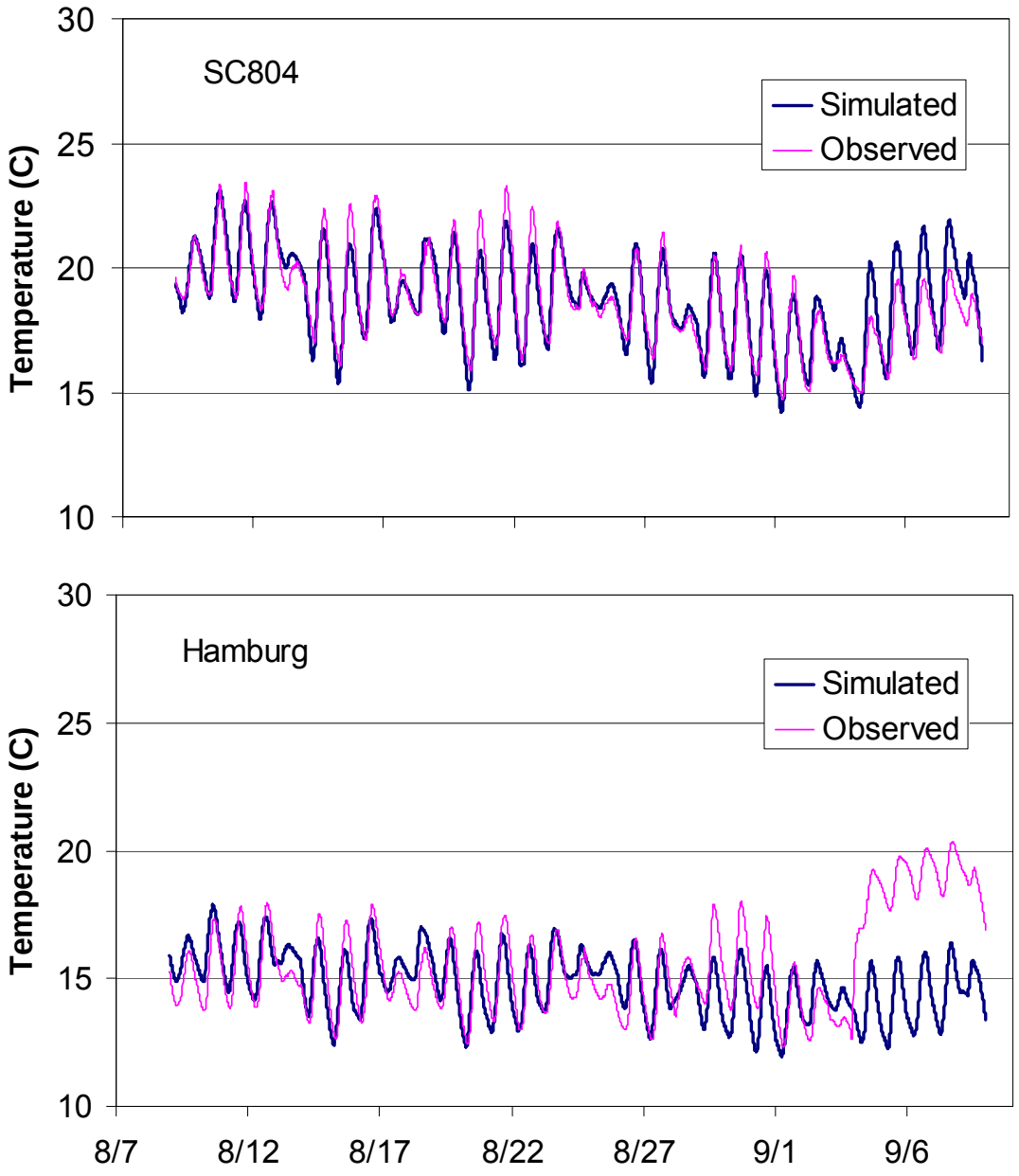

Figure 3.5. Simulated and observed stream temperature at the Hamburg Ave. and SC804 stations for the period 8/9/2006 to 9/8/2006. The RMSEs at the Hamburg and SC804 stations are 2.0 and 0.7 ºC, respectively. The observed temperature shifts upwards in September, likely due to a very flow condition.

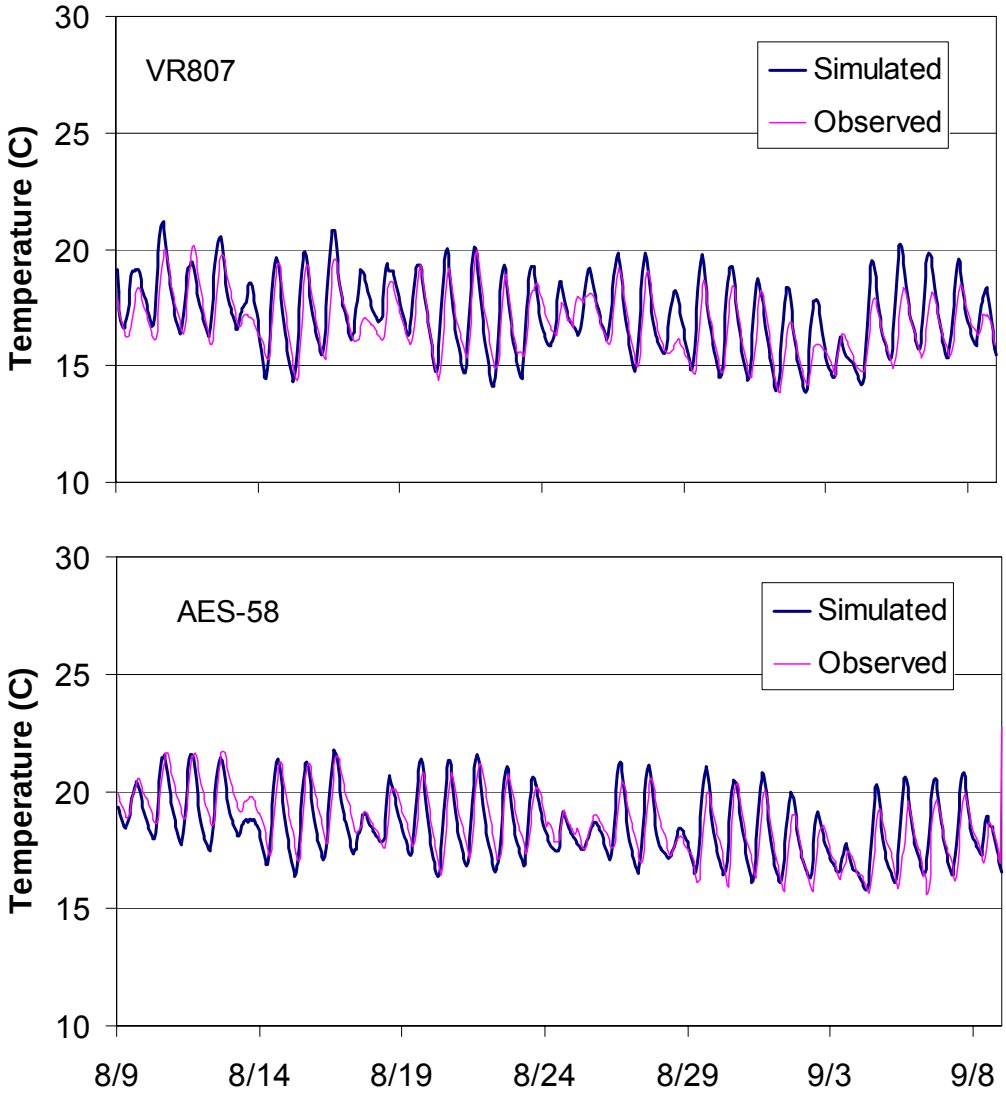

Figure 3.6. Simulated and observed stream temperature at the VR807 and AES-58 stations for the period 8/9/2006 to 9/8/2006. The RMSEs at VR807 andAES-58 are 1.1 and 1.0 ºC, respectively.

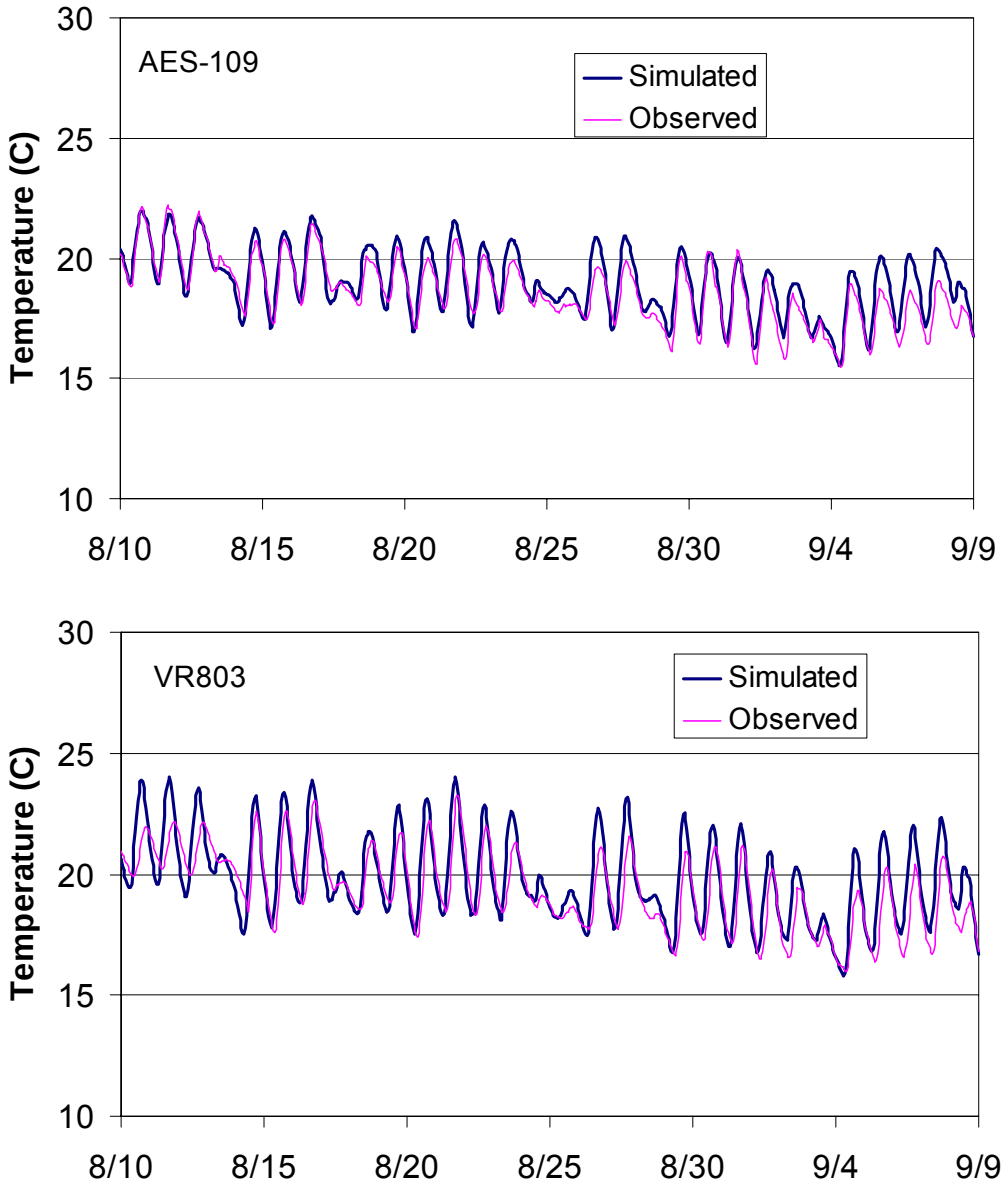

Figure 3.7. Simulated and observed stream temperature at the AES-109 and VR803 stations for the period 8/9/2006 to 9/8/2006. The RMSEs at VR803 andAES-109 are 1.1 and 0.7 ºC, respectively.

3.3 Temperature model for tributaries of the Vermillion River

Stream temperature models for tributaries of the Vermillion River were created in a similar manner to the main stem model. The period August 9 to September 8, 2006 was used as the calibration period for the tributary stream temperature models. Compared to the main stem, there are generally fewer stream flow and temperature observations available for the tributaries. As a result, the upstream boundary conditions for the temperature model had to be assumed in many cases (Table 3.7). Groundwater temperature was adjusted to obtain the best fit of simulated and observed daily mean stream temperature, using the flows previously established

groundwater inflow rates (Section xx). Like the model for the main stem, a parabolic function (Equation 3.17) was used to calculate the stream width based on the specified flow area from the flow solution. Shading and sheltering coefficients were adjusted to match simulated and observed diurnal temperature change. The resulting simulated temperature RMSEs are summarized in Table 3.9, ranging from 0.8 ºC for South Branch to 1.4 ºC for North Creek. A different calibration period was used for Middle Creek (July 1 to July 30, 2007), South Branch trib1 (Sept. 1 to Sept. 30, 2006), and South Creek trib2 (Sept. 11 to Sept. 30, 2006) due to the availability of stream temperature data. Reliable temperature calibration data was not available for North Creek trib1 and South Creek trib3. For these cases, the calibration parameters were set equal to similar, calibrated tributaries.

Table 3.6. Summary of specified upstream input temperatures and distributed groundwater temperatures for each tributary reach. Flow values are repeated from Table 2.3 for reference, and the location of each tributary is shown in Figure 2.1.

Reach	Upstream Input		Groundwater Input	
	Flow (cfs)	Temp. (ºC)	Flow (cfs)	Temp. (ºC)
Main Stem Trib3	0.25	18	0.25	12
Middle Creek	0.5	16	0.5	12
North Creek	0.5	18	5.25	15
North Creek Trib1	0.5	18	0.5	12
South Branch	0.5	16	5.1	14
South Branch Trib1	0.5	16	0.5	12
South Creek	0.25	18	5.6	15
South Creek Trib1	0.5	12	1.75	10
South Creek Trib2	0.25	18	0.4	12
South Creek Trib3	0.25	16	0.4	12

Table 3.7. Calibrated shading and wind sheltering coefficients for tributaries of the Vermillion River, and the RMSE of simulated stream temperature for the period August 9 to September 8, 2006.

Station	C_B ($m^{1/3}$)	Shading Coefficient	Sheltering Coefficient	RMSE (ºC)
Main Stem Trib3	3.7	0.85	0.85	
Middle Creek	5.5	0.85	0.85	1.5
North Creek	6.6	0.65	0.65	1.4
North Creek Trib1	5.5	0.7	0.7	
South Branch	6.6	0.45 – 0.85	0.45 – 0.85	0.8
South Branch Trib1	6.6	0.85	0.85	0.7
South Creek	3.7	0.5 – 0.75	0.5 – 0.75	1.2
South Creek Trib1	3.7	0.9	0.9	0.8
South Creek Trib2	5.5	0.8	0.8	1.2
South Creek Trib3	5.5	0.8	0.8	

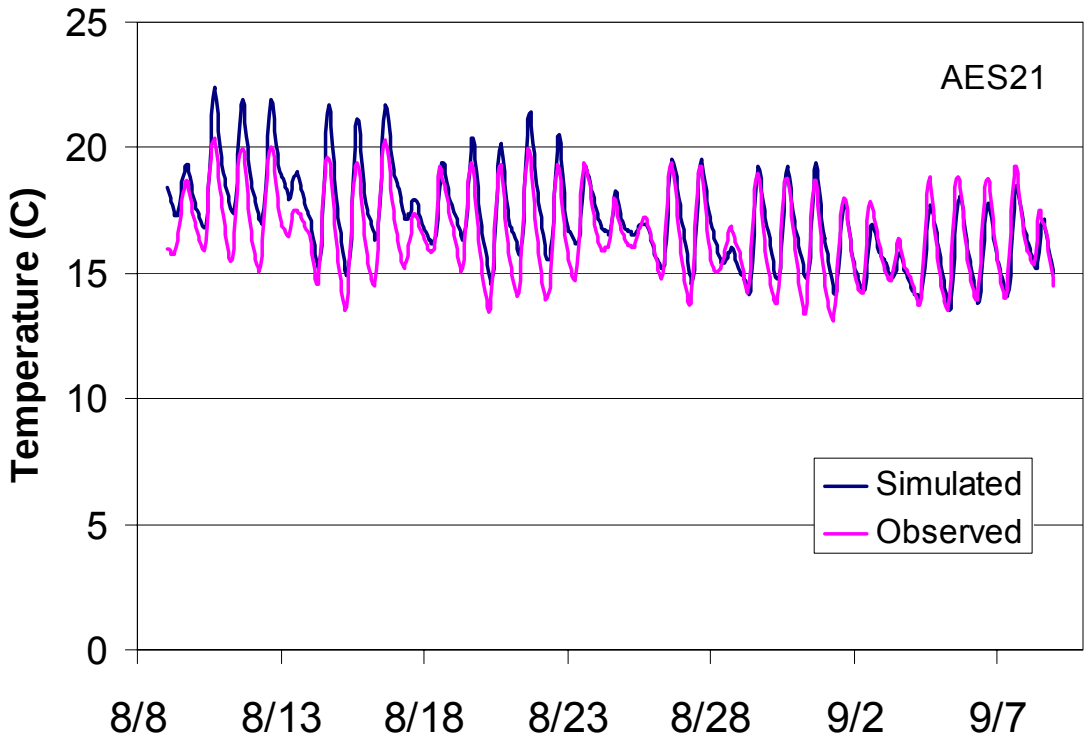

Figure 3.8. Simulated and observed stream temperature in South Branch at the AES-21 (SB802) station for the period 8/9/2006 to 9/8/2006. The RMSE is 0.8 ºC.

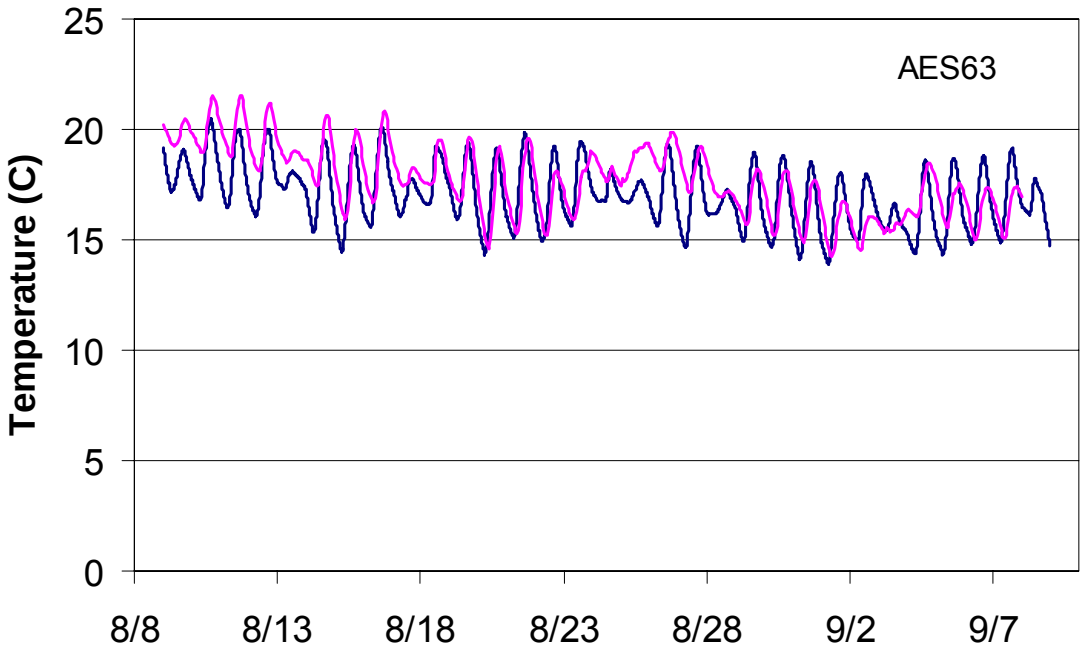

Figure 3.9. Simulated and observed stream temperature in North Creek at the AES-63 (MC801) station, downstream of the confluence with Middle Creek, for the period 8/9/2006 to 9/8/2006. The RMSE is 1.4 ºC.

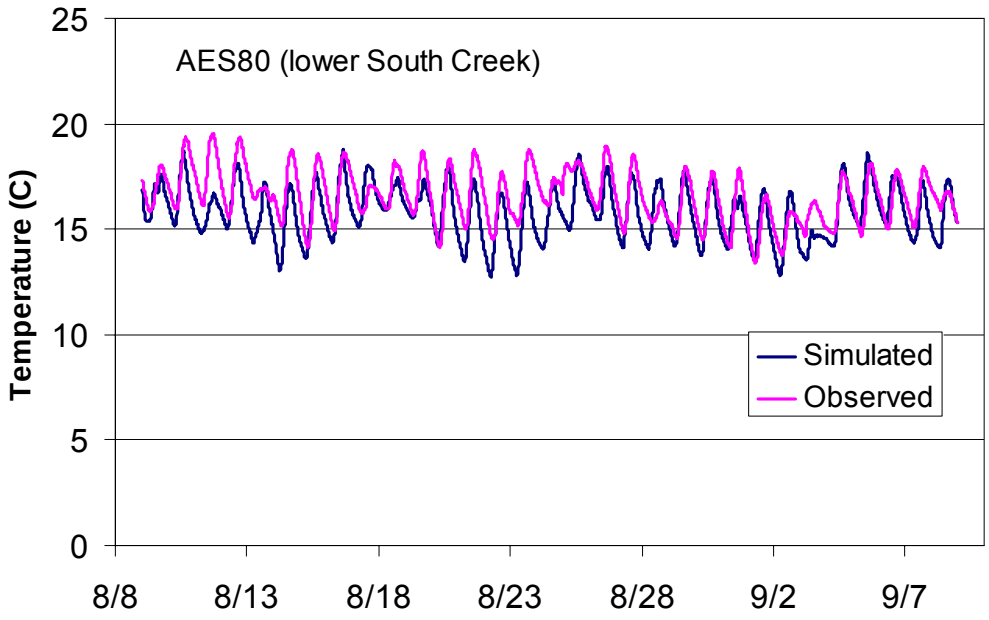

Figure 3.10. Simulated and observed stream temperature in South Creek at the AES-80 (SC-1) station for the period 8/9/2006 to 9/8/2006. The RMSE is 1.2 ºC.

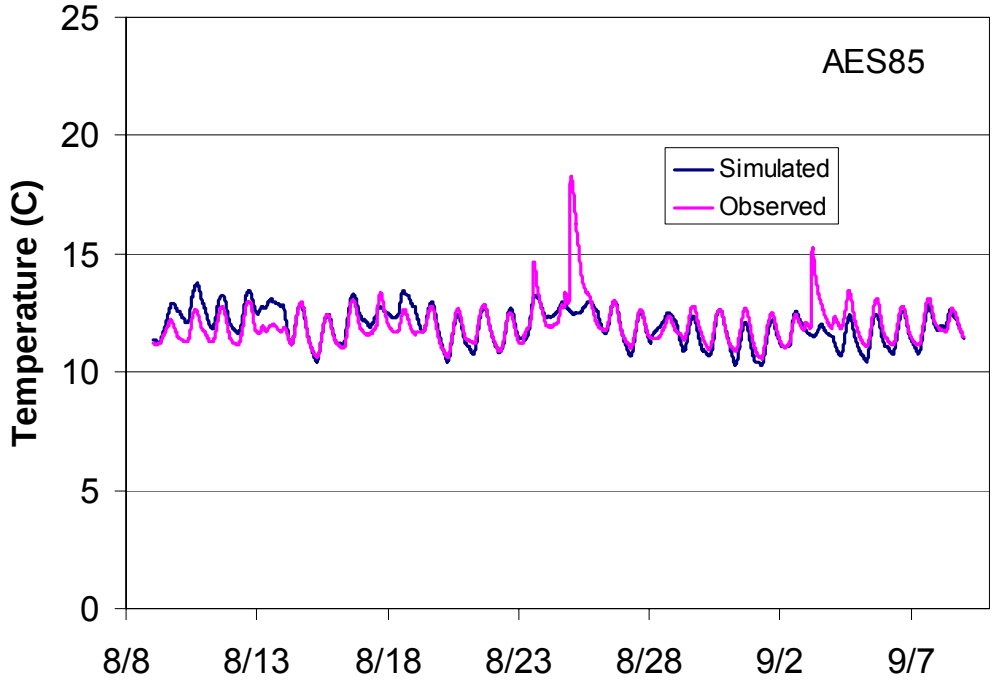

Figure 3.11. Simulated and observed stream temperature in South Creek Trib1 at the AES-85 (SC-1) station for the period 8/9/2006 to 9/8/2006. The RMSE is 0.8 ºC. The peaks in observed temperature on August 25 and September 3 are likely due to surface runoff inputs.

4. Summary and Conclusions

A stream flow and temperature model has been assembled for the Vermillion River, including the main stem from Dodd Avenue to Goodwin Avenue and a number of tributaries, including South Branch, South Creek, North Creek, and Middle Creek. The EPD-riv1 package was used to simulate stream flow, including distributed groundwater inputs. Simplified stream channel geometry was required to obtain converged flow solutions for unsteady low flows. A stream temperature model has been assembled based on the MNSTREM model (Sinokrot and Stefan 1993). The stream temperature model uses flow and flow area from the flow solver, along with observed climate data to calculate surface heat transfer. Groundwater inflows are an important component of both the flow and temperature model. For the Vermillion River, groundwater inflow rates were estimated from flow gaging sites, while groundwater temperatures were estimated by calibrating the stream temperature model. The calibrated combination of groundwater flow and temperature results in a good match of simulated and observed stream temperature, with RMSEs in the range of 0.75 to 2 ºC. However, uncertainty in the groundwater inflow rates lead to a corresponding uncertainty in the calibrated groundwater inflow temperature. Several smaller tributaries were included in the flow and temperature model that are not calibrated due to lack of field data. .For these cases, the calibration parameters were set equal to similar, calibrated tributaries.

The assembled flow and temperature model for the Vermillion River has been calibrated for baseflow conditions, and provides a starting point for analysis of surface runoff inputs during rainfall events for present and future land use scenarios.

Acknowledgments

This study was conducted with support from the Minnesota Pollution Control Agency, St. Paul, Minnesota, with Bruce Wilson as the project officer. Stream flow and temperature data were supplied by Travis Bistodeau of the Dakota County SWCD and the USGS. Precipitation data were obtained from Karen Jensen at the Met Council, and the University of Minnesota Rosemount Research and Outreach Center. Stream channel geometry was supplied bu Barr Engineering Company. The authors are grateful to these individuals and organizations for their cooperation.

References

Edinger, J., D.K. Brady and J.C. Geyer (1974). Heat exchange and transport in the environment. Report No. 14, Electric Power Research Institute, Cooling Water Discharge Research Project (RP-49), Palo Alto, CA, 125 pp.

Herb, W.R. and H.G. Stefan (2008). Analysis of Vermillion River Stream Flow Data (Dakota and Scott Counties, Minnesota). Project Report No. 514, St. Anthony Falls Laboratory, University of Minnesota, 28 pp.

Sinokrot, B.A. and Stefan, H.G. (1993). Stream Temperature Dynamics: Measurements and Modeling, *Water Resources Research* 29(7): 2299-2312.

US ACE (2008). HEC-RAS River Analysis System, version 4.0, U.S. Army Corps of Engineers, http://www.hec.usace.army.mil/software/hec-ras/.

US EPA (2005). One Dimensional Riverine Hydrodynamic and Water Quality Model, U.S. Environmental Protection Agency, http://www.epa.gov/ATHENS/wwqtsc/html/epd-riv1.html.

Appendix I: Surface Heat Flux Formulation

The net vertical heat transfer at the air-water interface includes components due to long wave radiation, short wave (solar) radiation, evaporation, and convection. The surface heat transfer formulations used in this study are based on those given by Edinger et al. (1968, 1974) for lake and reservoir surfaces.

The evaporative heat transfer formulation (Equation A.3) uses the aerodynamic method to enable simulations at hourly time steps or less. The evaporation and convection heat transfer components consider both forced convection, proportional to wind speed, and natural convection, related to the difference in temperature (density) of the air between the ground surface and the atmosphere. This differs from the formulations given in Edinger (1968, 1974), which do not take into account natural convection. The wind velocity at 10 m height (u_{10}) is scaled by a sheltering coefficient (CS_h) to take into account the effect of trees, buildings, and topographical features on surface wind velocity (u_s). Incoming atmospheric long wave radiation (h_{li}, Equation A.6) is calculated based on air temperature (T_a) and cloud cover (CR).

$$h_{atm} = h_{rad} - h_{evap} - h_{conv} - h_{ro} \quad (A.1)$$

$$h_{rad} = h_s + h_{li} - h_{lo} \quad (A.2)$$

$$h_{evap} = \rho_a L_v \left(C_{fc} u_s + C_{nc} \Delta\theta_v^{0.33}\right)\left(e_{sat} - e_a\right) \quad (A.3)$$

$$h_{conv} = \rho_a c_p \left(C_{fc} u_s + C_{nc} \Delta\theta_v^{0.33}\right)\left(T_s - T_a\right) \quad (A.4)$$

$$h_s = \left(1 - \alpha_s\right) R_s \quad (A.5)$$

$$h_{li} = \varepsilon\sigma\left(CR + 0.67 \cdot \left(1 - CR\right) e_a^{0.08}\right) T_{ak}^4 \quad (A.6)$$

$$h_{lo} = \varepsilon\sigma T_{sk}^4 \quad (A.7)$$

$$u_s = CS_h\, u_{10} \quad (A.8)$$

where h_{atm} is the total net surface heat transfer, h_{rad} is net radiation, h_s is the incoming short wave (solar) radiation, h_{evap} and h_{conv} are the evaporative and convective heat fluxes, respectively, ε and σ are the surface emissivity and the Stefan-Boltzmann constant, respectively, ρ_a is air density, c_p is the specific heat of water, L_v is the latent heat of vaporization, C_{fc} anf C_{nc} are coefficients for forced and natural convection, respectively, T_{ak} and T_{sk} are the absolute air and surface temperature (°K), respectively, e_{sat} and e_a are the saturated and ambient vapor pressure, respectively, $\Delta\theta_v$ is the different in virtual temperature between the surface and atmosphere, and α_s is the surface albedo. $\Delta\theta_v$ is set to zero for cases where the surface temperature is lower than air temperature.

Appendix II: Sediment Temperature Model Formulation

The vertical distribution of temperature is determined using a 1-D heat diffusion model. Since there are no heat sources in the sediment, the governing differential equation is given by:

$$\text{(A2.1)}\quad \frac{\partial T}{\partial t} + \frac{\partial}{\partial z}\left(D \frac{\partial T}{\partial z} \right) = 0$$

where T is temperature, t is time, z is vertical distance and D is the thermal diffusivity. The differential equation A.2.1 is discretized based on a control volume (Figure A.2.1) as follows:

$$\text{(A2.2)}\quad \frac{T_{i,j+1} - T_{i,j}}{\Delta t} = \frac{D}{\Delta z}\left(\left(\frac{\partial T}{\partial z} \right)_L - \left(\frac{\partial T}{\partial z} \right)_U \right) = \frac{D}{\Delta z}\left(\frac{(T_{i+1} - T_i)}{\delta z_i} - \frac{(T_i - T_{i-1})}{\delta z_{i-1}} \right)$$

The resulting equation for each nodal temperature is:

$$\text{(A2.3)}\quad A_i T_{i,j+1} = A_{i-1} T_{i-1,j+1} + A_{i+1} T_{i+1,j+1} + S$$

$$\text{(A2.4)}\quad A_i = \frac{\Delta z}{\Delta t} - A_{i-1} - A_{i+1}$$

$$\text{(A2.5)}\quad S = \frac{\Delta z}{\Delta t} T_{i,j}$$

$$\text{(A2.6)}\quad A_{i-1} = \frac{D}{\delta z_{i-1}}$$

$$\text{(A2.7)}\quad A_{i+1} = \frac{D}{\delta z_i}$$

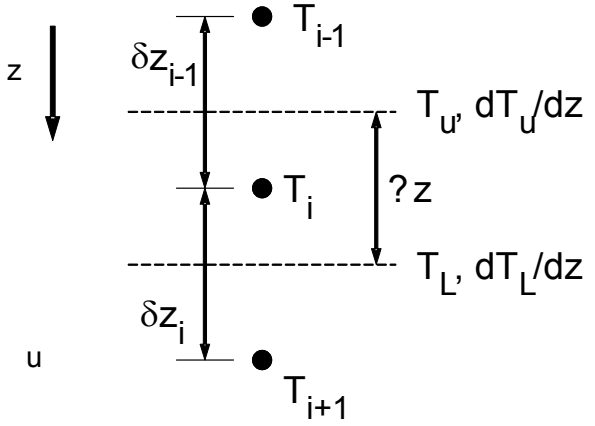

Figure A2.1. The finite difference control volume.

Boundary conditions are set at the sediment/water interface (sediment temperature = stream temperature) and at the bottom of the sediment column (adiabatic, $A_{i+1}=0$). The heat flux between the sediment and stream channel (h_{sed}) is calculated for each time step by integrating the change in temperature over the sediment column:

$$\text{(A2.8)}\quad h_{sed} = \rho c_p \sum_{i=1}^{n} \left(T_{i,j-1} - T_{i,j} \right) \cdot \Delta z_i$$

where j denotes the time step and n is the number of sediment layers.